Development of S-Band High Power Multi-Beam Klystron

by Ashish Bora

Submission date: 21-Nov-2020 01:39PM (UTC+0530)
Submission ID: 1449780224
File name: Seminar_Thesis.docx (1.53M)
Word count: 3025
Character count: 15221

Development of S-Band High Power Multi-Beam Klystron

ORIGINALITY REPORT

8%	0%	8%	0%
SIMILARITY INDEX	INTERNET SOURCES	PUBLICATIONS	STUDENT PAPERS

PRIMARY SOURCES

1	Shen, Bin, Yaogen Ding, Zhaochuan Zhang, Honghong Gu, Haibing Ding, Jing Cao, Caiying Wang, and Dongping Gao. "Research and Development of S-Band High Power Multibeam Klystron", IEEE Transactions on Electron Devices, 2014. Publication	6%
2	W.J. Pohl. "A simplified method for calculating klystron performance", IRE Transactions on Electron Devices, 1962 Publication	1%
3	Bin Shen, Yaogen Ding, Zhaochuan Zhang, Honghong Gu, Caiying Wang. "The design of S-band 1.5MW high power multi-beam klystron", 2015 IEEE International Vacuum Electronics Conference (IVEC), 2015 Publication	<1%
4	Y. Ding, B. Shen, S. Shi, J. Cao. "S-Band Multibeam Klystron With Bandwidth of 10%", IEEE Transactions on Electron Devices, 2005 Publication	<1%

Exclude quotes	On	Exclude matches	Off
Exclude bibliography	On		

Development of S-Band High Power Multi-beam Klystron

Ashish Bora, *M.Tech (RF and Microwave Engineering), IIT Kharagpur*

***Abstract*— A specific S-band high power klystron is designed and developed. The six cavities multibeam klystron (MBK) has been presented in this paper. Various factors such as perveance, space charge effects, beam current, gain, Q-factor has been discussed along with the designing of the klystron. The paper also discusses the effect of such parameters on the gain, efficiency, bandwidth, and output power of the klystron. There is also a brief explanation of the tradeoffs between low-noise and the high-power klystron in general, leading to an effect in the working lifetime of the klystron amplifiers.**

***Index Terms*—klystrons, Electron guns, oscillations, mode suppression, space charge.**

I. Introduction

HIGH-POWER multibeam klystron has become the heart of the modern broadband radar systems. Over the past decades, many companies and institutes have been developing klystrons to enhance output power, bandwidth, efficiency. The peak output power of the modern-day klystrons ranges from a few 100KW to MW. -However, the bandwidth has been extended nearly to 10-13% in recent years. The S-band MBK we are discussing in the literature has been developed with peak power of 1 MW and a bandwidth of 200 MHz. Generally, MBK can be categorized into two types based on the focusing used, one is the solenoid electromagnetic focusing, and the other is the periodic reversal of permanent magnetic focusing (PRPM). The MBK discussed here is a PRPM tube. The advantage of PRPM tube over solenoid focusing tube will be discussed later in the paper.

The paper is included with the simulations of the design for the S-band klystron. The phenomena that are observed while operation such as perveance, effects of space charge, decrease in the beam current, oscillations of the higher-order modes and electron reflections have been explained and methods to optimizing the above conditions have been presented in the paper.

II. Design Considerations and Specifications

The specifications for the design of the S-band MBK to be developed is shown in Table 1. A figure of the MBK that is implemented can be observed in Fig. 1.

1) To obtain a bandwidth of 200 MHz with an efficiency of more than 35% and gain of over 42 dB, the RF system includes a double-gap coupling cavity and buncher cavities that are operating in π-mode.

2) The current density of the cathode emitting has been kept under 15 A/cm^2 for extending the lifetime of the device (more than 1500 hours).

TABLE 1
Performance of S-Band MBK To Be Designed

Parameters	Values
Frequency range	S-band
Peak Power	$\geq$ 1 MW
Bandwidth	200 MHz
Efficiency	$\geq$35%
Beam Voltage	$\leq$ 40 kV
Gain	$\geq$ 42 dB
Lifetime	$\geq$ 1500 hours

Fig. 1. Fabricated MBK

3) A cooling system is used for both the body and the collector region of the MBK.

4) To achieve high (R/Q) and to realize the desired bandwidth, a fundamental mode TM01 for the system is adopted.

A. Electron Gun Design

A beam voltage of 35V and current of 71.5A are provided respectively. The MBK is provided with 24 beams to obtain a perveance of 11 µp.

The perveance of the klystron is decided by the electron gun geometric structure. The perveance in the klystron system is related to the space charge and has a direct effect on the working hours of the MBK. The lower is the perveance; the higher is the energy conversion efficiency since the space charge in the region is small. On the other hand, low perveance demands a higher voltage requirement. However, the higher voltage requirements increase the malfunction rate of the klystron device and leading to a reduction in the working hours of the MBK. Fig. 2 represents the curve for the working hours and the normalized perveance for the TH2100A klystron from the reference. The perveance dependence on the electron gun geometry can be supported by Child-Langmuir law which is widely used to describe the beam emission mechanism of the electron gun.

$$J = \frac{9}{4}\epsilon(2\eta)^{0.5}\frac{V^{3/2}}{x^2}$$

Parameter description:

J= Current Density on the cathode area

ϵ= Dielectric constant in a vacuum.

η= electron charge to mass ratio.

x= Distance from the cathode.

V= potential at position x.

$$I = PV^{3/2}$$

Combining the equations (1) and (2) we obtain:

$$P = \frac{4}{9}\frac{A\epsilon}{x^2}(2\eta)^{1/2} = 2.33 \times 10^{-6}\frac{A}{x^2}$$

The cathode area is dependent on the effective electron emission and changes for different work conditions.

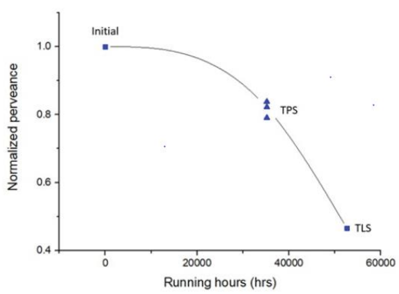

Fig. 2. Perveance change records of klystron for a TH2100A klystron.

The 24 beam klystron is necessary for extending power klystron generating capability at a specific frequency. The effective bandwidth, efficiency, gain and stability is observed to be equal to or greater than the single beam klystron. As mentioned above the required efficiency to be more than that of 35 % the use of multibeam in the device becomes necessary. The recent years conducted analysis shows that in broadband MBK in high frequencies band, the electromagnetic fields distributions in the cavities gap is different for different radial layers in the tube. The difference of the electromagnetic fields results to change in phase difference in the radial layers and thereby strongly affects the nature of bunching in the cavities. The effect on the bunching will lead to gain reduction and widening of bandwidth. Thus such factors also have to be taken by the designers so that optimum result can be obtained between bandwidth and output gain.

Each cathode has a diameter of 5mm. The basic requirement of a conventional cathode is uniform emission, high zero-field emission density and long life. Dimensional tolerances and cleanliness is also a factor which effects the performance of the cathode. The cathode affects the lifetime of the MBK as well. The cathode loading if gets higher reduces the lifetime of the klystron. Also, when the lower current density is used in the cathode, it operates at lower temperature and therefore, the lifetime of the MBK increases. The maximum cathode load in the solution for four MBK is 14.5 A/cm2. It can be simply termed as the current per unit area distribution along the radius of the cathode. The cathode load distribution is shown in Fig. 3.

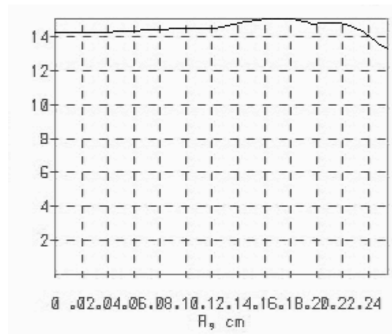

Fig. 3. Distribution of current along the cathode radius.

B. Beam Transporting and Focusing

The maximum magnetic field used along the axis and along the centre of the cathode is about 1130-1230 G and 60 G respectively. The magnetic field focusing system directed axially is shown in Fig. 4. which is a simulation of Arsenal-MSU. By adjusting the cathode plane magnetic field and peak magnetic field, a high transmission rate of the beam is obtained.

The period of the magnetic field and the period of the radial ripple of beam-trajectories must be matched to achieve the ideal beam transmission rate. The electron beam also acts as a factor to determine the noise of the MBK amplifier.

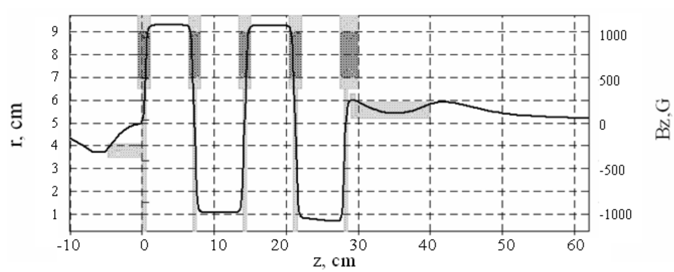

Fig. 4. PRPM focusing system axially.

The second part shows the characteristic impedance in Fig. 5. The characteristic impedance W depends on the total beam current, DC voltages and reduced radian plasma frequency. The low beam voltage region corresponds to the region of transmission of low characteristic impedance, and the high beam voltage region corresponds to a high characteristic impedance transmission line. The beam now is analogous to a section of a line transformer. Thus the analysis of the smith chart can fetch the result for optimum noise by analyzing the beam as a transmission line. The third part of Fig. 5 represents the noise currents that are estimated.

The MBK consists of five permanent magnets with radial magnetization for the focusing system. The focusing used here is PRPM focusing. The PRPM focusing is preferred over the solenoid electromagnetic focusing. A comparative study of both the type of focusing in the klystron has shown that the MBKs with the solenoidal focusing system of the coil has a high DC transmission rate of the beam and high RF beam transmission and are helps to obtain high power, but power supplies are required for focusing coils. The PRPM will reduce the need for power supplies at the cost of lower DC beam-transmission rate and lower RF beam-transmission rate. The PRPM makes the transmitter part more compact but with the limit is decreased for increasing the average output power. In the discussed case, both the methods were able to achieve the required specifications hence the reduction in the size and less power supply is an additional advantage of PRPM (periodic reversal permanent magnet) focusing of our MBK.

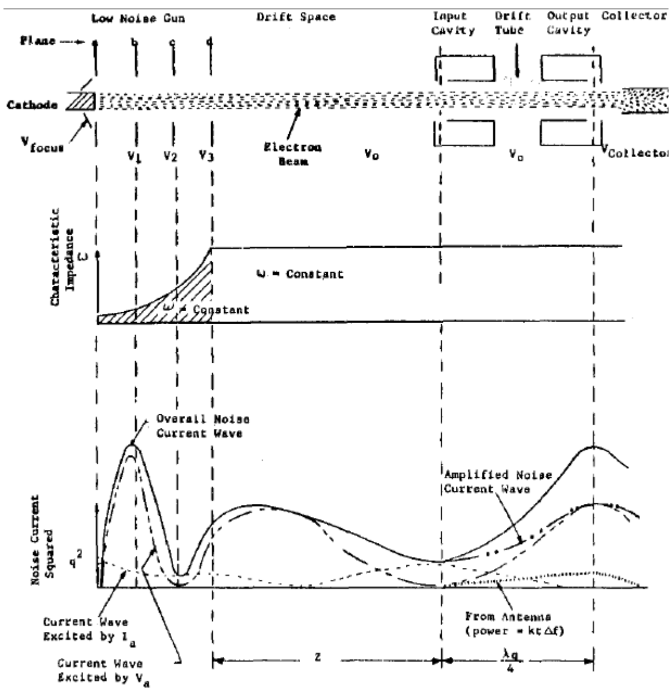

Fig. 5. Schematic for a low noise klystron amplifier

C. Circuit Design and Beam-Wave Interaction

The cavities are loaded with the material which properly suits the need the electrical and magnetic characteristics for microwave attenuating. The suitable dielectric suggested was FeSiAl with the dielectric constant of 110, with dielectric and permeability loss tangent of 0.2 and 2.46 respectively. Also, various specialized klystron computer codes can be used to design the beam-wave interaction and for the optimization of the parameters. Some of the klystron codes are 1-D klystron code, KLY6 and the 2.5 D klystron code, Arsenal-MSU are used for simulation of the wave and electron interaction in the tube.

The Q-factor, along with the drift length of the cavities, is optimized using the mentioned klystron codes. The required performance is obtained by varying the Q-factor, resonant frequency and the specified drift length. The dependence and optimization of the R/Q will be discussed in the following section in more detail.

D. Drift Length and Gain/Efficiency Compromise

The RF current in the final gap is largely dependent on the drift length and the extent of bunching at the penultimate cavity entrance.

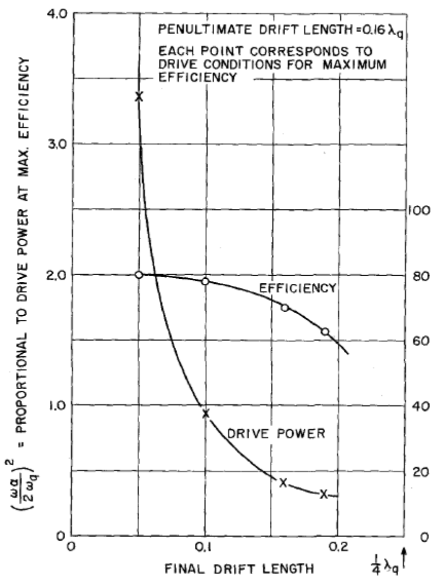

Fig. 6. The efficiency/gain compromise (three or more cavity)

Fig. 6 shows a clear picture of compromise done for either gain or efficiency of the beam RF power for all the multi-cavity tubes for practical purposes. The maximum efficiency of the voltage swing in the penultimate cavity is dependent on the drift distance. From Fig. 6, it can be observed that the range of 0.1λ-0.15λ is a good compromise for the drift length to attain an optimum gain and efficiency at the same time. Fig. 6 may be used for calculation of RF power for most of the practical operations. To achieve good gain drift length should be near to 0.15λ and for efficiency to be at its premium the drift length is desired to be near 0.1λ.

III. Higher-Order Modes and Oscillations

Few klystrons were designed before the MBK we are currently discussing, and the oscillation of higher modes was recorded under dc (no RF drive). Typically three klystrons from previous experiments show three spectral lines on the spectrometer when the beam voltage was taken to the operating beam voltage of 35kV from the zero voltage. At the range of 21-32 kV, an oscillation at 6207 MHz, and at a voltage range of 15-27 kV, the oscillation at 7300 MHz was observed.

A. Higher-Order Mode Oscillations

After analyzing the oscillations by the 3-D electromagnetic code, we found out that the oscillating modes are higher modes of the double gap cavity of the output. The simulation of the higher mode is shown in Fig. 7. The electron conductance can be observed by the Fig. 10 shown, which explains that the normalized electron conductance becomes negative when the beam voltage exceeds 22.5 kV. The output power of these modes has a significant effect on the MBK operation, although they are not large. The peak DC beam-transmission rate is limited, and the emitter beams current drops. The back bombardment is observed, and it is confirmed by the ion spots on the cathode as can be observed in Fig. 8 due to the reflected electrons.

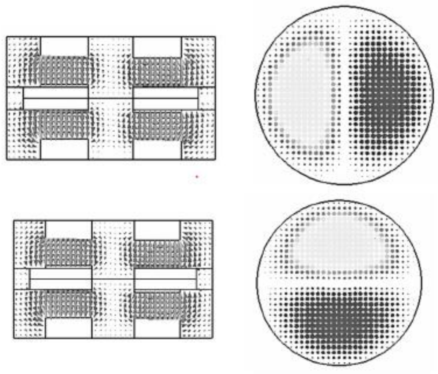

Fig. 7. Electric fields of $TM_{110\text{-}2\pi}$ for X-polarization (top) and Y-polarization (bottom).

Fig. 8. Ions spots on the module of the cathode.

The distribution at the back area confirms the presence of the higher-order modes TM_{110} 2π mode. The beam is disturbed by the negative electron beam and interacts at the drift tube's generating gas. Thus few ions get accelerated from the gas by the RF field of the oscillation modes and are bombarded at the cathode.

B. Suppression of Higher Order Modes

It was suggested to add absorbing cavities to suppress the higher-order mode oscillations. The absorbing cavities and their effects are shown in Fig. 9. One absorbing cavity for suppressing the TM_{110} 2π mode and TM_{110} 2π mode at the same time by coupling it through the coupling slot. The other

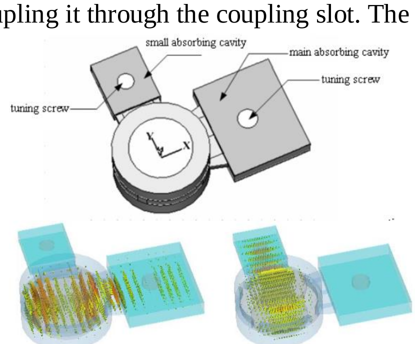

Fig. 9. Absorbing cavities made available for TM110 higher-order mode of X and Y polarization at left and right respectively.

An absorbing cavity is coupled through the wall of the coupling cavity which suppresses the mode TM_{110} 2π with the direction of polarization of the fields perpendicular to the output waveguides.

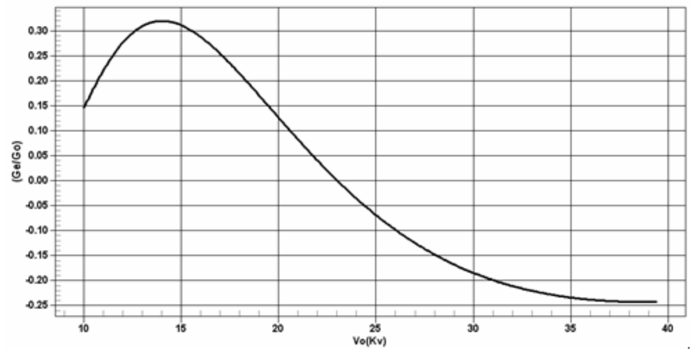

Fig. 10. Electron conductance normalized versus voltage of beam for the TM110-2π mode

IV. Input And Output Coupling Cavities

The interaction of beam and wave strongly takes place at the cavity gap. A high beam velocity modulation is supported by the high voltage for strong beam bunching, which results in RF extraction at the output cavity efficiently. The cavity gap voltage Vg is given by

$$V_g = M_{cf} Q_L \left(\frac{R}{Q}\right)(f_b I_b)$$

Parameter Description:
M_{cf}= Gap-coupling coefficient (a function of transit angle).
Q_L= Quality factor loaded at the cavity.
f_b= Bunching factor (fundamental).
I_b= Beam current (total).

The cavity R/Q is equal to $(\omega C_g)^{-1/2}$ where,
ω= Angular frequency of the cavity.
C_g= Gap capacitance.

The gap capacitance, for the lowest order, can be expressed as

$$C_g \alpha \ \frac{\pi r_g^2}{L_g}$$

r_g= radius of the nose gap.
L_g= Axial length of the gap.

It is clear from the equation mentioned above that to increase the bandwidth, the Q must be decreased and maximize R/Q, and hence the gap nose radius has to decrease, and the gap length has to be increased. The former choice is not any generally a good option for high compression electron guns, and the latter option is also not suggested because the longer gap decreases the gap coupling-coefficient. Therefore an alternative approach is to use interaction cavities (i.e., coupled cavities). The cavity gaps now have to be modelled as effective capacitances in series combination which can be represented as,

$$\frac{R}{Q} = \frac{1}{\omega C_{g1}} + \frac{1}{\omega C_{g2}} + \frac{1}{\omega C_{g3}} + \cdots + \frac{1}{\omega C_{gN}} \cong \frac{N}{\omega C_g}$$

N= Total number of gaps.

Here we assumed that all the cavities have equal gaps.

The thing that has to be noted is the increase the cavities also leads to an increase in the spurious oscillations. This particular phenomenon becomes a concern for high perveance broadband devices as in our case of the MBK. This is the reason we limit the cavities of two gaps.

V. Electrons Reflected From The Collector

A known phenomenon is the appearance of the reflected electrons which can lead to several problems in the device's operation, which includes 1) heating and damage of the cathode and walls of the tube. 2) drop in the efficiency, 3)unstable oscillations due to the feedback. The reflected electron hard to avoid because of the desire of the high-efficiency regime for the MBK.

A. Observation of Stray Output

Also, the stray output with or nearby the operating frequency of the MBK has been observed. The exits of the stray output have a significant influence on the normal operation of the klystron. After analyzing the cause of it was known to be the reflecting electrons and the secondary electrons caused by the interception of the gap head of the cavity and the electron beam. Thus reducing the reflected electrons becomes a serious matter of concern to avoid oscillations due to feedback and to reduce the stray output.

B. Space Charge

The MBK discussed at Fig. 11 has a beam voltage of 35kV; its electron trajectories can be observed. The minimum energy is 25.7 keV for the electron because of the space charge effects even though a voltage of 35kV has been applied. In the next case, a beam voltage of 10kV is applied then the electron potential turned out to be -8.99 kV which can be observed in Fig. 12. Some electrons must have returned back to the output cavity after getting de-accelerated greatly before entering in the collector under RF conditions.

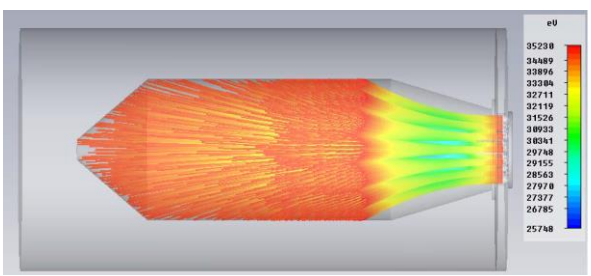

Fig. 11. Representation of beams diverging in the collector at a beam voltage of 35 kV.

To avoid the reflection of electrons, the shape of the collector is changed according to the potential drop of the entrance of the collector. Also, a metal rod was put on the centre of the piece of the magnet. This is expected to reduce the reflected electrons, as shown in Fig. 13.

VI. Test Results

The test results discussed, for output-window and filter-loaded

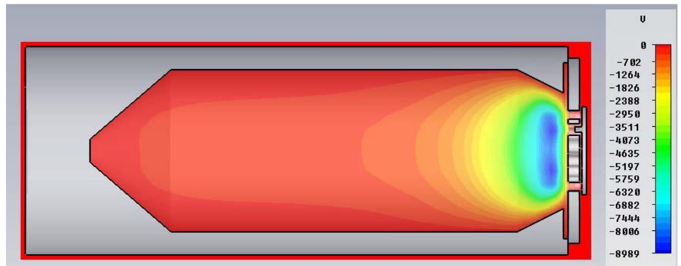

Fig. 12. Simulation of electrostatic potential in the collector of 10 kV voltage.

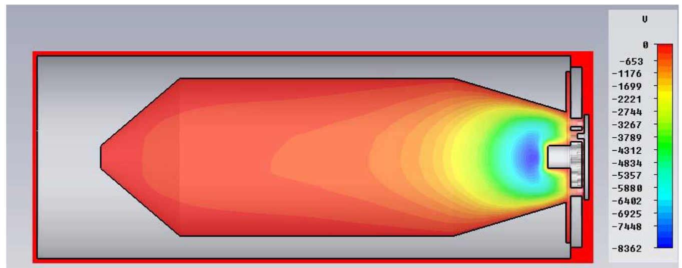

Fig. 13. Electrostatic potential simulated in collector with a metal rod with beam-voltage of 10 kV.

for double-gap cavity frequency characteristics shows strong agreement with the performed simulations. The manufactured MBK incorporates the solutions of the problems regarding the higher-order modes and the oscillations and the electron reflection in the tube. The transmission rate of more than 98% for the DC beam was observed. Neither the breakdown issues in the MBK was not observed, nor the decrease was seen in the DC operation of beam current that is emitted.

VII. Conclusion

We discussed the design, fabrication and the testing along with the simulation of the MBK for S-band with a peak output power of 1 MW. Various issues like space charge effects, higher-order modes, reflected electrons were discussed and also how to overcome these factors. The suppression of the higher mode of oscillation was carried out by adding the absorbing cavities. With a transmission rate of 98.5% for the beam, the improved MBK operates with stability under DC and RF conditions. The MBK generates a peak output power of 1MW, RF efficiency of 40%, and more than 47dB of RF gain over the bandwidth of 200MHz. Further research is processed to extend the bandwidth of the klystron and flatten the gain versus frequency curve of the MBK.

References

[1] Shen, Bin, Yaogen Ding, Zhaochuan Zhang, Honghong Gu, Haibing Ding, Jing Cao, Caiying Wang, and Dongping Gao. "Research and Development of S-Band High Power Multibeam Klystron", IEEE Transactions on Electron Devices, 2014.

[2] W.J. Pohl. "A simplified method for calculating klystron performance", IRE Transactions on Electron Devices, 1962

[3] Bin Shen, Yaogen Ding, Zhaochuan Zhang, Honghong Gu, Caiying Wang. "The design of Sband 1.5MW high power multi-beam klystron", 2015 IEEE International Vacuum Electronics Conference (IVEC), 2015

[4] Y. Ding, B. Shen, S. Shi, J. Cao. "S-Band Multibeam Klystron With Bandwidth of 10%", IEEE Transactions on Electron Devices, 2005

[5] B. Shen et al., "Research and Development of S-Band High Power Multibeam Klystron," in IEEE Transactions on Electron Devices, vol. 61, no. 6, pp. 1848-1853, June 2014, doi: 10.1109/TED.2014.2305712.

[6] K. Blotekjaer, "A proposed harmonic generator based on cyclotron waves," in IRE Transactions on Electron Devices, vol. 9, no. 1, pp. 27-32, Jan. 1962, doi: 10.1109/T-ED.1962.14884.